Mineral. Soc. Amer. Spec. Pap. **3**, 95–112 (1970).

ORIGIN OF THE GARNET PYROXENITE XENOLITHS AT SALT LAKE CRATER, OAHU[1]

MELVIN H. BEESON AND EVERETT D. JACKSON
U.S. Geological Survey, Menlo Park, California 94025

ABSTRACT

Mantle-derived garnet pyroxenite xenoliths are present in the eruptive material of a number of Honolulu Volcanic Series vents on Oahu, and are especially abundant in the nepheline basalt tuff at Salt Lake Crater. The textures of these xenoliths are dominated by unmixing caused by partial reequilibration; garnet and orthopyroxene have exsolved in large amounts from original clinopyroxene grains, and garnet and clinopyroxene have exsolved from original orthopyroxene grains. All of the xenoliths are now garnet pyroxenite, but textural reconstruction permits them to be divided into four original rock types: (1) clinopyroxenite; (2) websterite; (3) garnet websterite; and (4) garnet clinopyroxenite. Bulk chemical compositions of these xenoliths define a coherent, nearly linear trend intersecting the field of Honolulu lava compositions at one end. The trend in bulk chemistry, and similar trends in both observed and reconstructed mineral chemistry, are believed to have resulted from fractionation processes in the mantle. Comparison of whole rock compositions and mineralogy of the xenoliths with those expected for fractionation in the experimental system $CaSiO_3$-$MgSiO_3$-Al_2O_3 at 30 kilobars suggests that fractional fusion, rather than fractional crystallization, was the dominant process in the origin of the xenoliths.

INTRODUCTION

A great deal of interest has centered around the origin of the abundant xenoliths of coarse-grained mafic and ultramafic rocks found as broken fragments and blocks in the volcanic rocks of the Hawaiian Islands. It has long been recognized that these xenoliths represent fragments of the basement rocks beneath the Hawaiian chain (Goodrich, 1826), and most modern workers have concluded that many of them are hand samples of the oceanic upper mantle. It has been demonstrated that the petrologically heterogeneous xenoliths in Hawaiian volcanic rocks can be divided into groups spatially and temporally related to the major suites of basalts in which they occur (White, 1966; Jackson, 1968). From the point of view of mantle petrology, one of the most interesting groups of xenoliths occur in the nephelinitic suite of Macdonald and Katsura (1964), an undersaturated volcanic suite developed on a number of dissected tholeiite shields northwest of Molokai. Volcanic rocks of the nephelinitic suite on Oahu, named the Honolulu Volcanic Series by Stearns and Vaksvik (1935), are among the youngest and best known, and are especially notable for containing, among their diverse xenoliths, blocks of garnet pyroxenite, or "eclogite."

Garnet-bearing xenoliths were first recognized in the Salt Lake Tuff, one of the Honolulu vents, by Hitchcock in 1900. They were later found in other Honolulu vents by Jackson (1966) and Jackson and Wright (1970), but, so far as we know, these are the only occurrences of pyropic garnet-bearing rocks in the oceanic areas of the world. Nearly all recent investigators of these xenoliths agree that they have been derived from the upper mantle beneath Oahu and transported to the surface by ascending Honolulu magmas (for example Green, 1966; Kuno, 1969; O'Hara, 1969); their bearing on theories of an eclogitic oceanic mantle is most important. Three hypotheses of origin of these Hawaiian xenoliths have been extensively discussed: (1) the garnet pyroxenites represent basaltic liquids equilibrated at mantle *T-P* conditions (Yoder and Tilley, 1962; Kuno, 1969); (2) the garnet pyroxenites were formed as Al-rich clinopyroxene or garnet-pyroxene cumulates (Tilley and Yoder, 1964; Kuno, 1964; Green, 1966; O'Hara, 1969); and (3) the garnet pyroxenites were of part parental to basalt and in part refractory residua from which basalt had been extracted (Jackson and Wright, 1970). Most investigators agree that, subsequent to their formation, the xenoliths were reequilibrated at either lower temperature or higher pressure conditions, which resulted in considerable unmixing of the aluminous pyroxenes. It seems probable that such reequilibration took place before incorporation of the xenoliths in the basaltic rocks that carried them to the surface (Green, 1966, Jackson and Wright, 1970). The purpose of this paper is to reexamine these ideas in the light of new data on the mineralogy and petrology of the garnet pyroxenite xenoliths.

FIELD SETTING

The Pleistocene to Holocene Honolulu Volcanic Series was erupted from about 37 vents scattered over the 2.3 m.y. old Koolau tholeiite shield (McDougall, 1964) which forms the backbone of southeastern Oahu. Xenoliths occur in the flows or ejecta from 18 of these vents, but Jackson and Wright (1970) have shown that garnet-bearing types occur only around the apron of the shield. They are largest and most abundant at Salt Lake Crater (Fig. 1), a maar-like tuff cone near Pearl Harbor, and all of the samples described in this paper occur as loose blocks and xenolith-cored bombs embedded in tuff at that locality.

Two kinds of garnet-bearing xenoliths are found in the Salt Lake Tuff: (1) garnet pyroxenites that are commonly interbanded with deformed lherzolites in single blocks; and (2) garnet lherzolites that, thus far, have only been found as single unbanded xenoliths. The relations between these two types have been discussed by Jackson and Wright (1970); in this paper we will describe and discuss only the first group of rocks. Further, we wish to confine our attention almost entirely to the garnet pyroxenite xenoliths themselves, although it should be emphasized

[1] Publication authorized by the Director, U. S. Geological Survey.

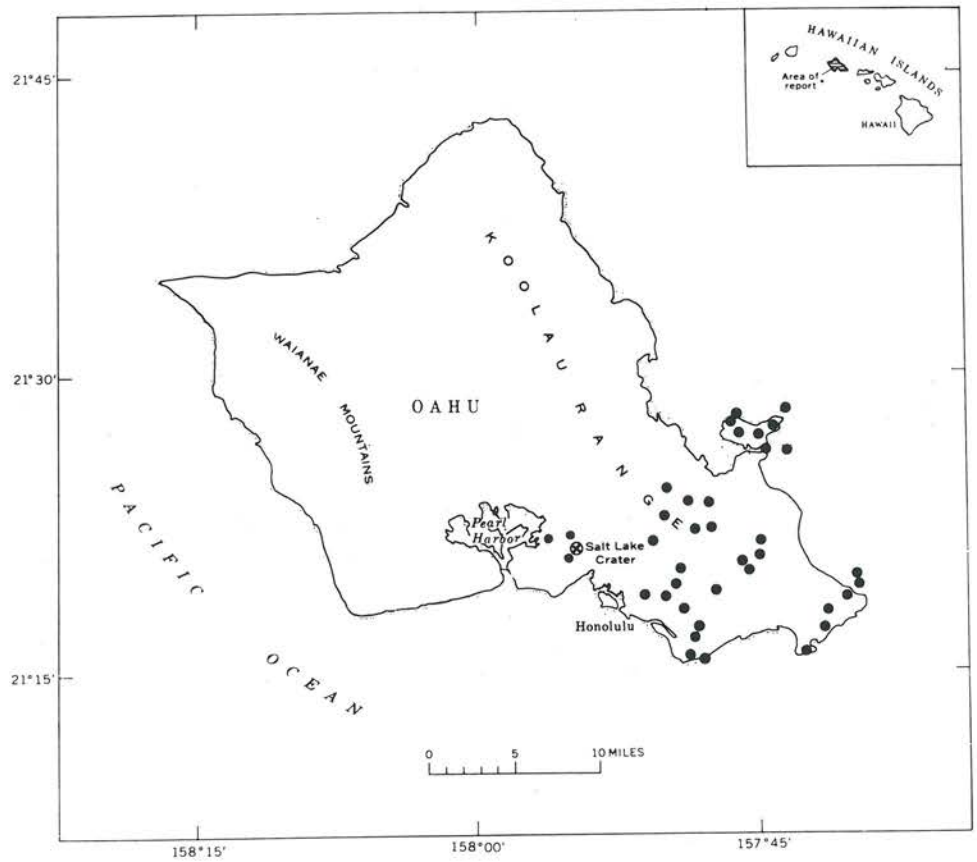

FIG. 1. Source vents of the Honolulu Volcanic Series on Oahu. Salt Lake Crater vent, source of all samples of this study, marked by ⊗.

that their ultimate origin cannot be divorced from that of the lherzolites with which they are commonly interbanded. Nevertheless, the present textures and mineral assemblages of the garnet pyroxenites were formed subsequent to the penetrative solid deformation that affected the lherzolites, and it is this period of post-deformational history that we wish to pursue.

PETROGRAPHY OF THE XENOLITHS

Textures. Textures of the garnet pyroxenites are generally dominated by unmixing. Yoder and Tilley (1962) observed copious quantities of orthopyroxene exsolved from clinopyroxene in these rocks, and Green (1966) observed garnet exsolved from clinopyroxene as well. The prevalence of unmixing textures is striking, and the unmixed phases are so abundant that the original textures of the rocks are nearly obscured. Exsolution textures are not, however, ubiquitous. We have been able to distinguish four basic textural types of garnet pyroxenite xenoliths:

1. Garnet websterites that are principally composed of large (3 to 5 mm) grains of clinopyroxene, which have exsolved both orthopyroxene and garnet (Fig. 2A). All of the orthopyroxene in these rocks occurs as exsolution plates or blebs; these commonly favor (100) or (001) planes in the host, but are more commonly myrmekitic (Fig. 2B). Garnet occurs either as exsolution lamellae in clinopyroxene (Fig. 2C, D) or as clearly unmixed grain boundary blebs. These rocks appear originally to have been clinopyroxenites (essentially single-phase rocks) that were subsequently partially reequilibrated at subsolidus conditions. If these rocks ever had cumulus textures, no evidence of them remains.

2. Garnet websterites that are principally composed of clinopyroxene grains like those of type 1, but that also contain 5–10 percent of large (1.5 to 3 mm) discrete orthopyroxene grains. In these rocks the clinopyroxene grains have exsolved orthopyroxene and garnet, and the large orthopyroxene grains have exsolved clinopyroxene (on 100) and garnet, though both exsolved minerals are much less abundant than in the clinopyroxene. Spinel is a minor but ubiquitous phase, and is locally mantled by garnet. These rocks appear to have been originally websterites (essentially two-phase rocks, plus minor spinel), that were partially re-equilibrated at subsolidus conditions. Again no evidence of original cumulus textures has been seen.

3. Garnet websterites that are principally composed of large irregular grains of clinopyroxene that have exsolved orthopyroxene and garnet, much less abundant large orthopyroxene grains that have exsolved clinopyroxene and garnet, and discrete 2.5 to 5 mm grains of garnet.

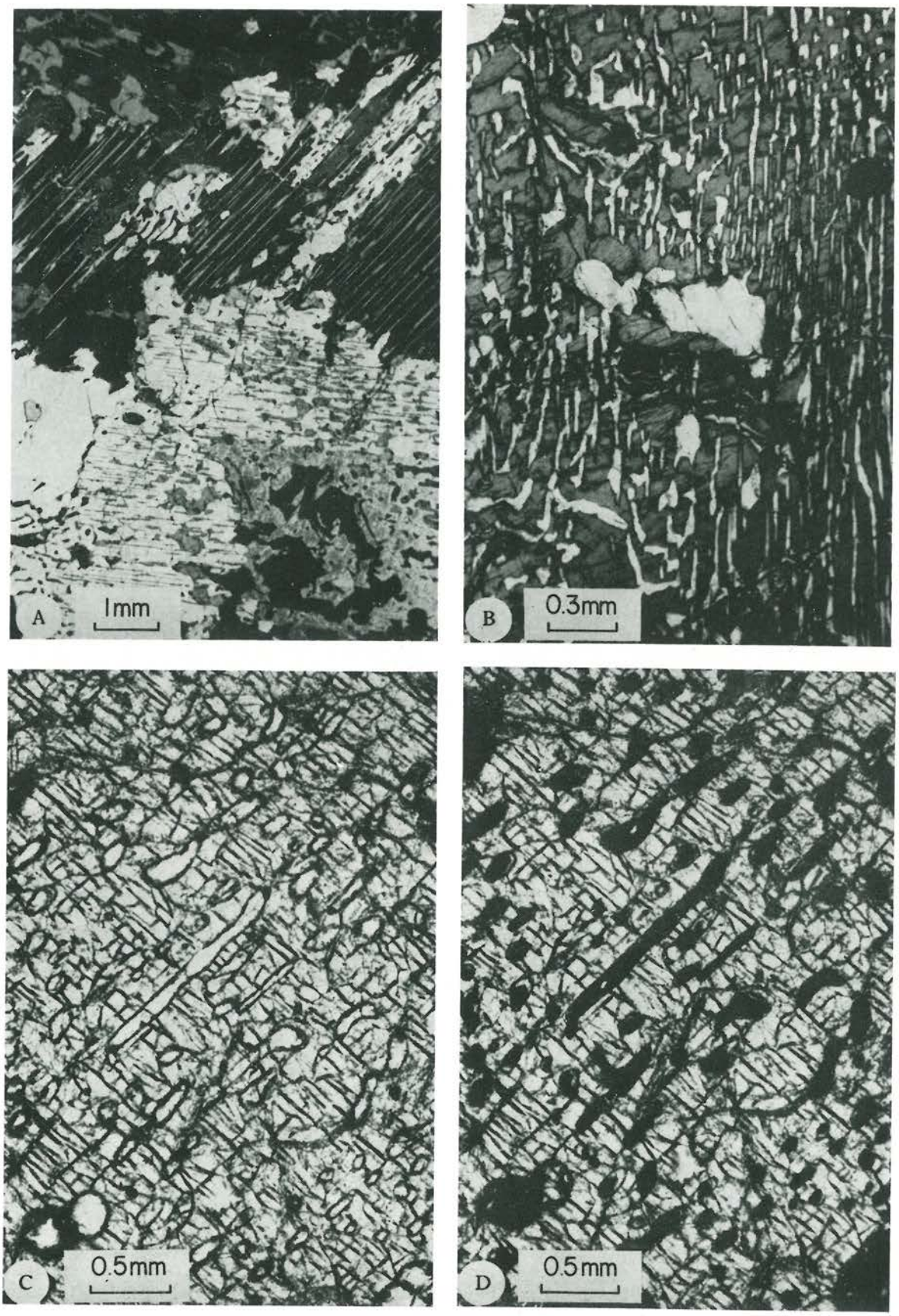

FIG. 2. Unmixing textures in type 1 garnet pyroxenite: A. Clinopyroxene grains with exsolution lamellae of orthopyroxene and garnet, crossed nicols; B. Typical myrmekitic exsolution of orthopyroxene from clinopyroxene, crossed nicols; C. Garnet exsolution lamellae in clinopyroxene, plane light; D. Same view as 2C, crossed nicols.

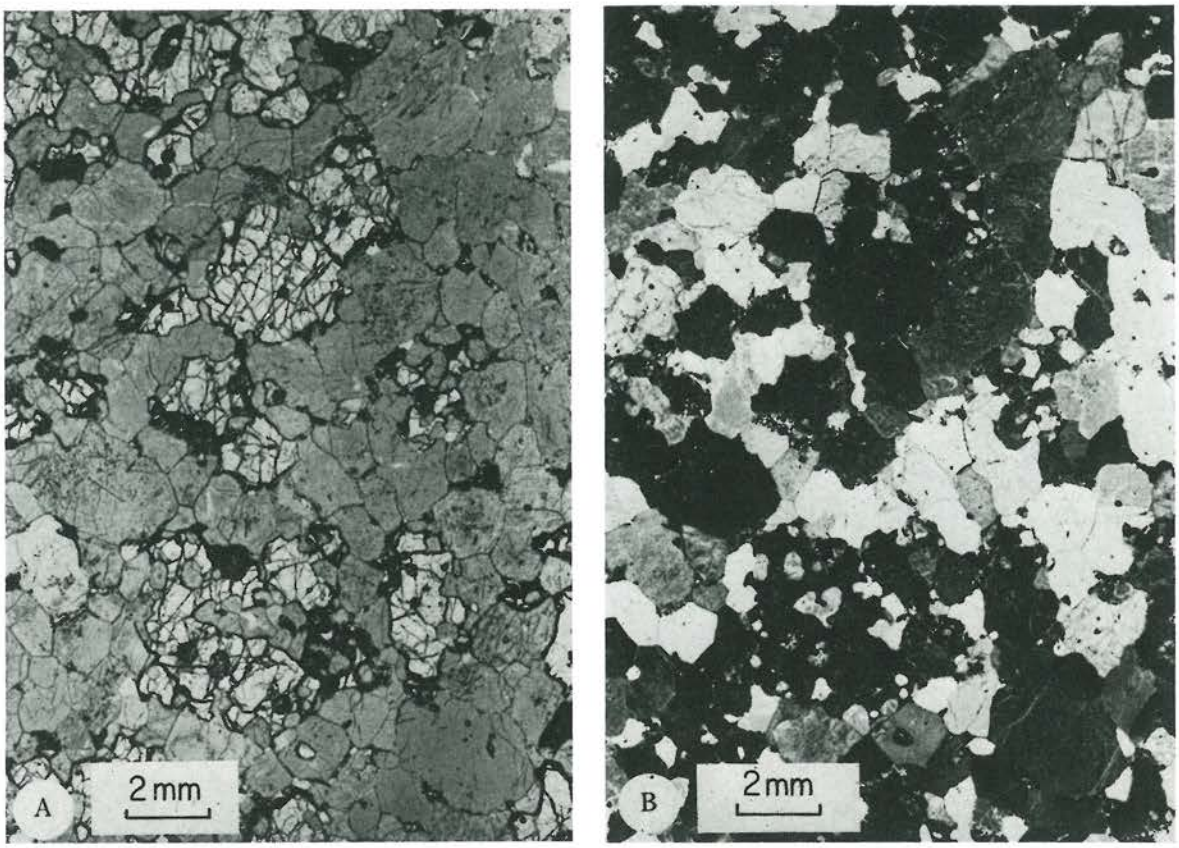

FIG. 3. "Igneous" texture of type 4 garnet pyroxenite: A. Garnet occurs as large discrete grains, not as exsolution lamellae or blebs from clinopyroxene, plane light; B. Same view as 3B, crossed nicols. Large clinopyroxene grains show no evidence of unmixing textures.

Spinel is always present in these rocks, and is invariably separated from clinopyroxene by rims of garnet. The garnet, then, has three textural relations: (1) exsolution lamellae and blebs in both pyroxenes; (2) continuous reaction rims on spinel (Green, 1966; Jackson and Wright, 1970); and (3) discrete and probably primary grains in the rocks. Type 3 rocks appear to have orginally consisted of the three major phases clinopyroxene, orthopyroxene, and garnet (plus minor spinel), with clinopyroxene much in excess of orthopyroxene, and with garnet and spinel both more abundant than in type 1 or 2 rocks. The rocks have also been partially reequilibrated, not only by unmixing, but by reaction of clinopyroxene and spinel to form more garnet. No indication of original cumulus textures has been seen.

4. Garnet clinopyroxenites that are principally composed of large (1 to 4 mm) grains of clinopyroxene and garnet, with minor magnetite-ilmenite. The clinopyroxene grains show no exsolution phenomena of any kind (Fig. 3A, B). These rocks do not appear to have cumulus textures, but somewhat resemble MacGregor's (1969) "igneous" eclogites from the Roberts Victor kimberlite pipe in South Africa. Presumably the rocks represent an original garnet-clinopyroxene (two phase plus minor magnetite-ilmenite) assemblage; if they have been subsequently reequilibrated they show no textural evidence of it.

All of the garnet pyroxenites in the Honolulu Volcanic Series appear to be minor variants of these four types, and all, in one xenolith or another, have been found interbanded with lherzolite. They are not uncommonly interbanded with each other, except that garnet clinopyroxenite has not been observed in the same hand specimen with orthopyroxene-bearing pyroxenite types. Some type 2, and especially type 3 xenoliths, contain a few iron-rich olivine grains (White, 1966) located near spinel-garnet contacts, and presumably are products of the clinopyroxene-spinel reaction.

We selected five rocks, one of each type (two of type 2) from our large collection of Salt Lake xenoliths for detailed study. It is possible that these do not represent the entire range of variation; in fact, the bulk chemistry of two of the Salt Lake xenoliths analyzed by Kuno (1969) suggests that some type 1 xenoliths may contain more exsolved orthopyroxene than our sample of that type. All other Honolulu garnet pyroxenite xenoliths that have been investigated (Yoder and Tilley, 1962; Macdonald and Katsura, 1964;

TABLE 1. MODES OF ANALYZED XENOLITHS

Mineral	68SAL-6			68SAL-24			68SAL-26			68SAL-7			68SAL-11		
	Observed	Bulk	Reconstr.	Observed	Bulk	Reconstr.	Observed	Bulk	Reconstr.	Observed	Bulk	Reconstr.	Observed	Bulk	Reconstr.
Olivine	—			tr	tr	tr	tr	tr	tr	tr	tr	tr	0.4	0.4	0.4
Orthopyroxene	—	22.0		5.8	19.9	6.0	5.6	16.2	5.7	7.9	8.7	10.0	—		
Opx exsolved from cpx	22.0			14.1			10.6			0.8			—		
Clinopyroxene	70.2	70.5	99.8	67.9	68.1	93.0	65.5	65.6	90.9	52.6	53.2	66.9	61.2	61.2	61.2
Cpx exsolved from opx	0.3			0.2			0.1			0.6		19.4	—		
Garnet	—	7.3		—	11.2		—	16.2		19.4	34.4		36.5	36.5	36.5
Gar exsolved from cpx	7.3			11.0			14.8			13.5			—		
Gar exsolved from opx	—			—			—			1.5			—		
Gar reacted from spinel	—			0.2			1.4			—			—		
Spinel	tr	tr	tr	0.6	0.6	0.8	1.4	1.4	2.8	3.0	3.0	3.0	0.5	0.5	0.5
Ilmenite	—			—			—			—			0.3	0.3	0.3
Magnetite	—			—			—			—			0.6	0.6	0.6
Phlogopite	0.2	0.2	0.2	0.1	0.1	0.1	0.5	0.5	0.5	tr	tr	tr	tr	tr	tr
Amphibole	—			—			—			0.5	0.5	0.5	—		
Sulfide minerals	tr	tr	tr	0.1	0.1	0.1	0.1	0.1	0.1	0.2	0.2	0.2	0.5	0.5	0.5
Total	100.0	100.0	100.0	100.0	100.0	100.0	100.0	100.0	100.0	100.0	100.0	100.0	100.0	100.0	100.0

White, 1966; Green, 1966; Lovering and White, 1969; Kuno, 1969) appear to fall within the textural and compositional limits of those we investigated.

Modes. Most of the garnet pyroxenite xenoliths contain more than one textural variety of clinopyroxene, orthopyroxene, and garnet. In making modes of the rocks we tabulated these textural varieties separately, and the data are given for the five xenoliths in Table 1. The "observed mode" in this table is that actually counted from thin sections, with the textural distinctions intact. These values were then combined in two ways: (1) the total amounts of each mineral in the five rocks were combined, regardless of texture into a "bulk mode" (Table 1); and (2) the total amounts of exsolved or reacted material, no matter what its present mineralogy, were combined back into the large discrete grains from which it was exsolved or reacted, to form a "reconstructed mode" (Table 1). The bulk modes provide the present partially reequilibrated, subsolidus mineral assemblages of the rocks, and the reconstructed modes give the mineral assemblages at some time before reequilibration, as far back in time as the textures permit us to observe.

The bulk and reconstructed modes are plotted on one face of the garnet peridotite tetrahedron (Jackson, 1968) in Figure 4, where the bulk and reconstructed modes of each xenolith are connected by tie lines. The type 1 xenolith (68SAL-6) is a clinopyroxene-rich garnet websterite, but all of its orthopyroxene and garnet are exsolved, and it appears originally to have been a clinopyroxenite. The two type 2 xenoliths (68SAL-24 and 68SAL-26) are garnet websterites, but were originally websterites. The type 3 xenolith (68SAL-7) is a garnet websterite, and appears always to have been a three-phase rock, although its total garnet and orthopyroxene contents have been increased by subsolidus exsolution. The type 4 xenolith (68SAL-11) does not show obvious reequilibration features, and its bulk and reconstructed modes are the same.

CHEMISTRY OF THE XENOLITHS

Rock compositions. Bulk wet-chemical analyses were made by the method of Peck (1964). Analytical results and CIPW norms of our five investigated xenoliths are given in Table 2. All are undersaturated with respect to quartz, but none contains normative nepheline. All five contain large amounts of normative feldspar and olivine, although in the actual rocks these constituents are represented in the higher pressure phases garnet and aluminous pyroxene. All five xenoliths are roughly "basaltic," although none contains enough K_2O, P_2O_5, or, to a lesser extent, TiO_2 to be completely representative of basalts.

The relationship between the bulk chemistry of the five xenoliths and the bulk chemistry of Oahuan basalts is shown in Figure 5. It is apparent that the garnet pyroxenite xenoliths are not chemically equivalent, nor do they appear related in any way, to the Koolau tholeiites that build the major part of the shield. Only one of the xenoliths (68SAL-11, a type 4 xenolith) appears chemically equivalent to any of the younger Honolulu basalts. That xenolith plots with Honolulu basanites, even though it contains no normative nepheline. The other four analyzed xenoliths also seem clearly related to the Honolulu rather than Koolau basalts, and they form a more or less linear path away from the center of the Honolulu compositional field toward a point midway between clinopyroxene and orthopyroxene mineral compositions. The bulk composition of our type 3 xenolith (68SAL-7) lies nearest to that of the basalts, our two type 2 xenoliths (68SAL-24 and 26) are intermediate, and our type 1 xenolith (68SAL-6) is farthest away.

Mineral compositions. Mineral analyses were made with an A.R.L. EMX electron microprobe using natural mineral standards. All data were corrected for drift, background, matrix absorption, characteristic fluorescence, and atomic number effects (Beeson, 1967; Beaman and Isasi, 1970).

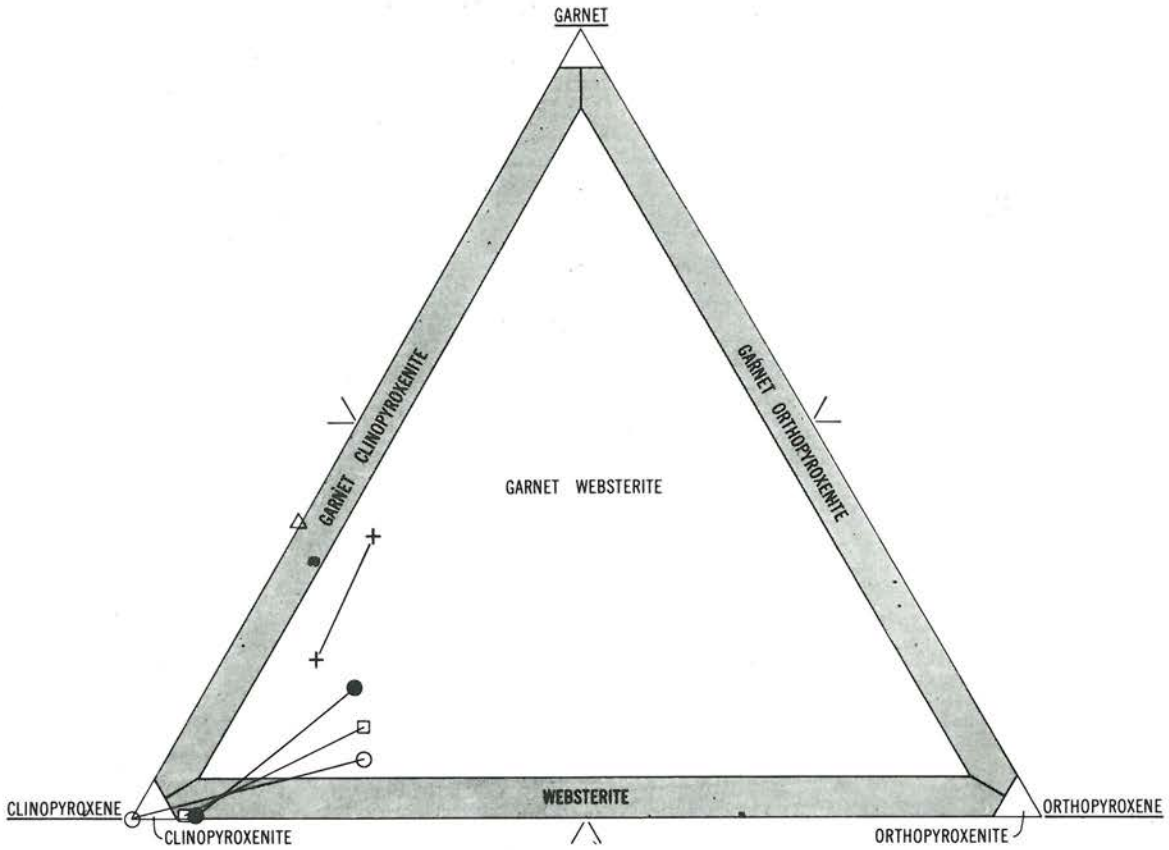

FIG. 4. Bulk and reconstructed modes of garnet pyroxenite xenoliths. Arrows lead from bulk to reconstructed mode. Sample numbers: open circle, 68SAL-6; square, 68SAL-24; shaded circle, 68SAL-26; plus, 68SAL-7; and triangle, 68SAL-11.

Major element values are precise within ± 2 relative percent (as defined by Boyd, 1969), minor elements within 5–10 relative percent. Compositional data are given in Tables 3, 4 and 5; averages of analyzed material are given in the "observed" columns, recombined analytical data in the "bulk" and "reconstructed" columns. The same significant figures are retained in recombined data for consistency. Use of the microprobe made it possible for us to analyze individual mineral compositions in different textural configurations.

Compositions of clinopyroxenes, which are common to all five rocks, are given in Table 3. In general, observed compositions of the large clinopyroxene hosts contain more CaO and Al_2O_3, particularly IV coordinated Al^{3+}, than clinopyroxene exsolved from orthopyroxene in the same rocks. Large discrete grains are therefore measurably richer in Ca-Tschermak's molecule than that unmixed from orthopyroxene, although Fe/Mg ratios are about the same. In general, to obtain the average compositions of minerals in each rock, the observed analytical values were weighted according to the observed textural modes in Table 1, and arithmetically combined into "bulk compositions"[1] of Tables 3, 4, and 5. In comparing bulk (in this case host) clinopyroxene compositions from type 1 through type 4 xenoliths one finds a general increase in Al_2O_3, 'FeO', Na_2O, and TiO_2, and a general decrease in CaO, MgO, and Cr_2O_3. This corresponds to an increase in hedenbergite and jadeite components.

The strong unmixing textures permit us to recombine the observed mineral compositions in still another way: obviously exsolved orthopyroxene and garnet in host clinopyroxene were separately analyzed (Tables 4 and 5) and arithmetically combined according to the textural modes into "reconstructed compositions" (Table 3). These reconstructed values give the original compositions of the clinopyroxenes in these rocks before partial reequilibration; in fact, as far back in their histories as the textures permit us to see. In the case of our type 1 xenolith, which texturally appears to have been a clinopyroxenite, the whole-rock composition (Table 2) is simply calculated as a pyroxene in Table 3. The reconstructed compositions for the other four xenoliths have been calculated from the modes and observed mineral compositions, according to the proportions given in Table 1. Incorporation of ex-

[1] In the case of the clinopyroxene compositions, the amount of clinopyroxene exsolved from orthopyroxene is so small compared with the amount of host clinopyroxene that the bulk and host compositions are the same.

solved orthopyroxene and garnet into the reconstructed compostions causes a general marked decrease in CaO content and an increase in Al_2O_3, MgO, and 'FeO'. Whereas differences between bulk (host) clinopyroxene compositions among the five xenoliths were small, differences after reconstruction are larger and more systematic. In going from type 1 to type 4 reconstructed pyroxenes, Al_2O_3, 'FeO', CaO, Na_2O, and TiO_2 increase, and MgO and Cr_2O_3 decrease markedly. The change is not simply an increase in Ca-Tschermak's molecule, although that is one component of it.

Compositions of orthopyroxenes from the four rocks that contain them are given in Table 4. In the two rocks where both host and exsolved orthopyroxenes were analyzed (68SAL-24, 26), compositions are quite similar, except that Al_2O_3 tends to be somewhat richer in the exsolved phases. In comparing the bulk orthopyroxene compositions in the three xenoliths that contain discrete grains of orthopyroxene, in this case going from type 2 to type 3 xenoliths, one finds a small increase in Na_2O and TiO_2, and a decrease in Al_2O_3 and Cr_2O_3. The direction of change is suggestive of that in the clinopyroxenes, except that Al_2O_3 in the orthopyroxenes definitely changes in the opposite direction. No systematic changes in 'FeO', MgO, or CaO are apparent.

Reconstructed compositions of orthopyroxenes show much less change from bulk compositions than do those of clinopyroxenes, because the orthopyroxene textures indicate a good deal less recognizable exsolution. The effect, in general, is to increase CaO, since clinopyroxene (from Table 3) is being incorporated, and to increase Al_2O_3 as well, due to incorporation of garnet (from Table 3). The change in reconstructed orthopyroxene compositions in going from type 2 to type 3 xenoliths is in the same direction as in clinopyroxene: Al_2O_3, CaO, Na_2O, and TiO_2 increase; MgO and Cr_2O_3 decrease. Again, the change involves an increase in Ca-Tschermak's molecule, as well as some jadeitic component.

Compositions of garnets are given in Table 5. Garnets are pyrope-rich and show a good deal less chemical change with textural type than do pyroxenes in the same rocks. The bulk compositions are therefore not very different from the observed compositions. We have not attempted to reconstruct garnet compositions. Three of the five xenoliths had no original garnet at all, and a fourth shows no textural evidence of reequilibration. It would be interesting to reconstruct the pyroxene-spinel compositions involved in the garnet reaction rims, but impossible at this time. In going from type 1 to type 4 xenoliths, the bulk garnet compositions increase in Fe/Mg and decrease slightly in CaO. More specifically, the almandine component increases at the expense of both grossularite and pyrope components in going from type 1 to type 3 xenoliths and at the expense of pyrope alone in going from type 3 to 4 xenoliths.

All of the mineral analyses show cation excesses when reduced to ions per formula. While this could be due to analytical error, the amounts of Fe_2O_3 in the whole-rock analyses suggest that ferric iron is present in all three minerals. We analyzed the opaque oxides and phlogopite of these rocks, although they are not reported in this paper, and calculated chemical modes of the rocks by the method of Wright and Doherty (1970). No reasonable amount of these two minerals can supply the Fe_2O_3 content of the rocks. We therefore calculated the amounts of ferric iron needed to restore cation totals to theoretical numbers per formula, and the FeO and Fe_2O_3 values are reported in Tables 3, 4, and 5. Chemical modes using these mineral analyses virtually reproduced the measured modes. We do not, however, wish to place undue reliance on the Fe^{2+}–Fe^{3+} values calculated from cation totals, and have used them in only one of the succeeding diagrams (Fig. 7).

TABLE 2. BULK COMPOSITIONS OF ANALYSED XENOLITHS

	D102105 68SAL-6	D102107 68SAL-24	D102109 68SAL-26	D102106 68SAL-7	D102222 68SAL-11
SiO_2	50.20	49.52	48.42	45.58	44.57
Al_2O_3	8.37	9.31	9.46	13.69	13.61
Fe_2O_3	1.58	2.26	3.14	3.76	4.17
FeO	5.72	5.44	7.27	5.85	8.49
MgO	19.00	17.97	16.85	16.09	13.34
CaO	13.28	12.90	12.15	11.78	11.42
Na_2O	0.87	1.17	1.41	1.27	1.69
K_2O	0.02	0.04	0.01	0.02	0.02
H_2O^+	0.05	0.17	0.09	0.35	0.29
H_2O^-	0.04	0.16	0.10	0.32	0.14
TiO_2	0.51	0.42	0.70	0.80	1.76
P_2O_5	0.02	0.03	0.03	0.03	0.02
MnO	0.16	0.16	0.17	0.16	0.21
CO_2	0.03	0.10	0.01	0.09	0.03
Cl	0.00	0.00	0.00	0.00	0.00
F	0.01	0.01	0.01	0.01	0.01
S	0.07	0.05	0.07	0.05	n.d.
Cr_2O_3	0.24	0.35	0.22	0.12	0.06
NiO	0.10	0.09	0.07	0.06	0.04
Subtotal	100.27	100.15	100.18	100.03	99.87
less 0	0.04	0.03	0.04	0.03	0.00
Total	100.23	100.12	100.14	100.00	99.87
[a] 100 Mg/Mg+Fe^{2+}	85	85	81	83	74
Norms (CIPW)					
q	—	—	—	—	—
or	0.12	0.24	0.06	0.12	0.12
ab	7.36	9.90	11.93	10.75	14.30
an	18.87	20.03	19.45	31.60	29.49
ne	—	—	—	—	—
di wo	19.47	17.99	16.91	10.87	11.18
di en	14.78	13.77	12.40	8.34	7.92
di fs	2.69	2.33	2.91	1.38	2.30
hy en	16.68	14.31	10.93	7.54	3.04
hy fs	3.04	2.42	2.57	1.25	0.88
ol fo	11.12	11.69	13.06	16.95	15.61
ol fa	2.23	2.18	3.78	3.08	5.00
mt	2.29	3.28	4.55	5.45	6.05
il	0.97	0.80	1.33	1.52	3.34
cm	0.35	0.52	0.32	0.18	0.09
cc	0.07	0.23	0.02	0.21	0.07
ap	0.05	0.07	0.07	0.07	0.05
fr	0.02	0.02	0.02	0.02	0.02
Total	100.11	99.78	100.31	99.33	99.46

[a] Mole percent.

DISCUSSION OF RESULTS

Comparison of assemblages. The occurrence of garnet pyroxenite xenoliths that contain pyrope-rich garnet and

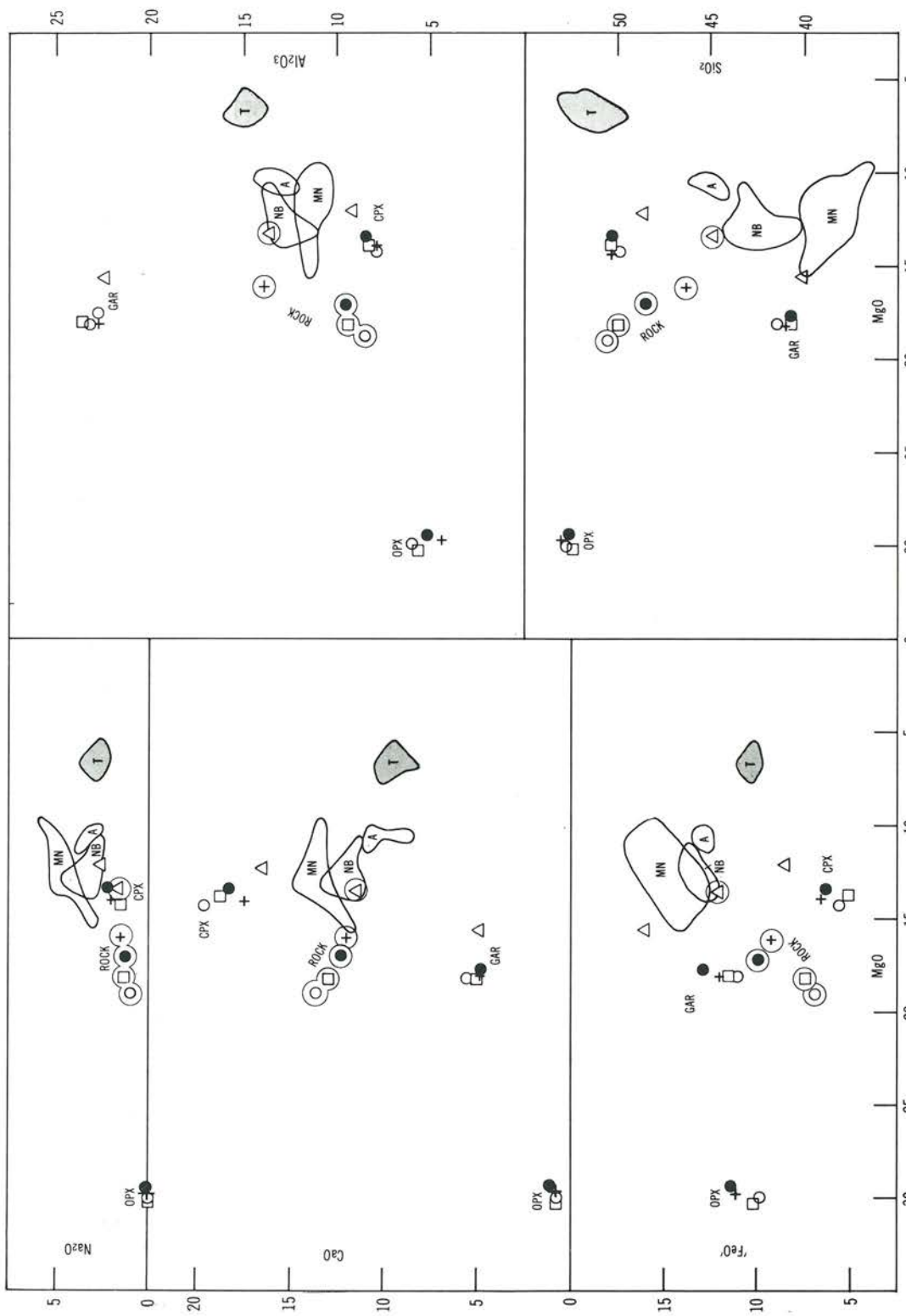

FIG. 5. Magnesia variation diagram for basalts and xenoliths. Oxides given in weight percent. Field of Koolau Series tholeiites is shown by the darkly shaded areas labeled T. Rocks of the Honolulu Volcanic Series have been divided into melilite-nepheline basalts, nepheline basalts, and alkali basalts lightly shaded and labeled MN, NB and A respectively. OPX indicates orthopyroxene mineral compositions; CPX, clinopyroxenes; GAR, garnet. "Rock" indicates whole rock chemical composition of xenoliths. Symbols (circles, squares, pluses, etc.) identify sample numbers, and are the same as given in Fig. 4. Mineral compositions are plotted with plain symbols; rock compositions with circled symbols.

TABLE 3. COMPOSITIONS OF CLINOPYROXENES

	68SAL-6			68SAL-24			68SAL-26			68SAL-7		68SAL-11
	Host[a] observed	Exsolved[b] observed	Re-constr.[c]	Host[a] observed	Exsolved[b] observed	Re-constr.[d]	Host[a] observed	Exsolved[b] observed	Re-constr.[d]	Host[a] observed	Re-constr.[d]	Observed
SiO_2	49.24	50.07	50.20	51.19	51.61	50.31	50.46	52.89	48.97	49.12	47.31	48.60
Al_2O_3	7.82	7.38	8.37	8.40	8.11	9.96	8.39	7.21	10.67	7.66	10.99	9.31
'FeO'	5.64	5.94	7.14	5.24	5.75	6.78	6.51	6.49	8.24	6.65	3.08	8.86
MgO	13.96	14.59	19.00	13.94	15.19	16.88	13.69	14.04	16.18	13.75	14.86	12.10
CaO	19.22	18.65	13.28	19.15	18.89	14.59	18.20	18.30	13.84	17.16	14.23	16.53
Na_2O	1.45	1.42	0.87	1.96	1.98	1.43	2.15	2.06	1.54	2.17	1.67	2.69
K_2O	0.04	0.04	0.02	—	—	—	0.01	0.01	0.01	—	—	0.01
TiO_2	0.84	0.93	0.51	0.57	0.61	0.45	0.87	0.83	0.68	1.17	0.97	1.69
Cr_2O_3	n.d.	n.d.	0.24	0.47	0.43	0.42	0.32	0.33	0.29	0.10	0.10	0.06
MnO	0.12	0.12	0.16	0.10	0.10	0.15	0.10	0.10	0.16	0.11	0.16	0.10
Total	98.33	99.14	99.79	101.02	102.67	100.95	100.70	102.26	100.58	97.89	98.37	99.95
Calc. FeO	3.26		5.72	3.26		5.09	3.41		5.28	3.21	4.78	4.39
Calc. Fe_2O_3	2.65		1.58	2.20		1.88	3.45		3.29	3.82	3.67	4.97
Total	98.60		99.95	101.24		101.14	101.05		100.91	98.27	98.74	100.45
Number of ions on the basis of 6 oxygens												
Si	1.833	1.846	1.817	1.847	1.836	1.804	1.835	1.887	1.774	1.838	1.757	1.799
Al^{IV}	0.167	0.154	0.183	0.153	0.164	0.196	0.165	0.113	0.226	0.162	0.243	0.201
Al^{VI}	0.176	0.166	0.174	0.204	0.176	0.225	0.195	0.190	0.229	0.176	0.238	0.205
Cr	—	—	0.007	0.013	0.012	0.012	0.009	0.009	0.008	0.003	0.003	0.002
Ti	0.024	0.026	0.014	0.015	0.016	0.012	0.024	0.022	0.019	0.033	0.027	0.047
Mg	0.774	0.802	1.025	0.750	0.805	0.902	0.742	0.746	0.874	0.767	0.823	0.658
Fe^{2+}	0.176	0.183	0.216	0.158	0.171	0.203	0.198	0.194	0.250	0.208	0.251	0.274
Mn	0.004	0.004	0.005	0.003	0.003	0.005	0.003	0.003	0.005	0.004	0.005	0.003
Ca	0.766	0.737	0.515	0.740	0.720	0.561	0.709	0.699	0.537	0.688	0.566	0.655
Na	0.105	0.102	0.061	0.137	0.137	0.099	0.152	0.143	0.108	0.158	0.120	0.193
K	0.002	0.002	0.001	—	—	—	0.001	0.001	0.001	—	—	0.001
Total	4.03	4.02	4.02	4.02	4.04	4.02	4.03	4.01	4.03	4.04	4.03	4.05
Total using FeO_3 & Fe_2O_3	4.00		4.00	4.00		4.00	4.00		4.00	4.00	4.00	4.00
Ca[e]	44.7	42.8	29.3	44.9	42.4	33.6	43.0	42.7	32.4	41.4	34.5	41.0
Mg[e]	45.1	46.6	58.4	45.5	47.5	54.2	45.0	45.5	52.6	46.1	50.2	41.8
Fe^{2+}[e]	10.2	10.6	12.3	9.6	10.1	12.2	12.0	11.8	15.0	12.5	15.3	17.2
Fe^{2+}/Mg[f]	0.227	0.228	0.211	0.211	0.212	0.225	0.267	0.260	0.286	0.271	0.305	0.411
Al_2O_3[g]	8.6		9.0	9.3		10.8	9.4		11.7	8.8	12.4	10.8
(Mg, 'Fe')SiO_3[g]	47.4		61.6	46.8		56.3	48.5		56.9	50.3	54.5	49.5
$CaSiO_3$[g]	44.0		29.4	43.9		32.9	42.1		31.4	40.9	33.1	39.7

[a] observed and bulk composition are the same
[b] clinopyroxene exsolved from orthopyroxene
[c] rock analysis calculated as clinopyroxene (see reconstructed mode in Table 1).
[d] observed clinopyroxene composition plus exsolved phases (see reconstructed mode in Table 1).
[e] ionic percent; total iron as Fe^{2+}.
[f] ionic ratio; total iron as Fe^{2+}.
[g] weight percent; total iron expressed as equivalent weight of Mg.
Analyst: M. H. Beeson.

aluminous pyroxenes have been reported in nephelinite tuff or kimberlite pipes from South Africa (Rickwood and others, 1968; Kushiro and Aoki, 1968; MacGregor, 1969; Boyd and Nixon, 1970), North Africa (Girod, 1967), Australia (Lovering and White, 1969), Kenya (Saggerson, 1968), and New Zealand (Mason, 1966; Dickey, 1968). These xenoliths are commonly associated with olivine-rich lherzolites or harzburgites and are generally considered to have been derived from the upper mantle. Furthermore, xenoliths at many of these localities are similar to garnet pyroxenite-lherzolite assemblages in periodotite massifs also believed to have once been mantle residents (Kornprobst, 1969; Dickey, 1970). Experimental studies of garnet-pyroxene assemblages at high pressures (O'Hara, 1963; Davis, 1963; Davis and Boyd, 1966; Green, 1966; Kushiro and Yoder, 1966; Green and Ringwood, 1967a,b,

TABLE 4. COMPOSITIONS OF ORTHOPYROXENES

	68SAL-6	68SAL-24				68SAL-26				68SAL-7	
	Exsolved observed	Host observed	Exsolved[b] observed	Calculated[c] Bulk	Reconstr.[d]	Host observed	Exsolved[b] observed	Calculated[c] Bulk	Reconstr.[d]	Host[a] observed	Reconstr.[d]
SiO_2	53.24	50.40	53.87	52.86	50.44	50.59	51.55	51.22	50.63	51.98	49.96
Al_2O_3	5.99	5.53	6.13	5.96	5.62	4.41	5.51	5.13	4.46	4.34	7.61
'FeO'	10.09	10.33	9.84	9.97	10.13	11.53	11.31	11.39	11.44	11.06	11.11
MgO	30.36	29.79	29.91	29.88	29.29	29.17	28.79	28.92	28.89	29.28	26.50
CaO	0.65	0.61	0.66	0.64	1.24	0.82	0.80	0.81	1.13	0.80	2.41
Na_2O	0.09	0.12	0.12	0.12	0.18	0.15	0.16	0.16	0.18	0.17	0.26
K_2O	0.03	—	0.01	—	—	—	—	—	—	—	—
TiO_2	0.23	0.14	0.12	0.13	0.16	0.21	0.24	0.23	0.22	0.28	0.34
Cr_2O_3	n.d.	0.21	0.20	0.19	0.22	0.14	0.16	0.15	0.14	0.04	0.05
MnO	0.17	0.15	0.15	0.15	0.15	0.15	0.15	0.15	0.15	0.13	0.16
Total	100.85	97.28	101.01	99.90	97.42	97.17	98.67	98.15	97.24	98.08	98.40
Calc. FeO	8.44			8.62	5.72			8.11	6.88	8.36	8.82
Calc. Fe_2O_3	1.83			1.50	4.90			3.65	5.07	3.00	2.55
Total	101.03			100.05	97.93			98.52	97.75	98.38	98.66
Number of ions on the basis of 6 oxygens											
Si	1.857	1.833	1.871	1.860	1.833	1.854	1.853	1.853	1.855	1.877	1.809
Al^{IV}	0.143	0.167	0.129	0.140	0.167	0.146	0.147	0.147	0.145	0.123	0.191
Al^{VI}	0.103	0.070	0.122	0.108	0.074	0.044	0.087	0.072	0.047	0.062	0.134
Cr	—	0.006	0.006	0.005	0.006	0.004	0.005	0.004	0.004	0.001	0.001
Ti	0.006	0.004	0.003	0.003	0.004	0.006	0.007	0.006	0.006	0.008	0.009
Mg	1.578	1.615	1.458	1.567	1.587	1.593	1.543	1.560	1.578	1.576	1.430
Fe^{2+}	0.294	0.314	0.286	0.293	0.308	0.353	0.340	0.345	0.351	0.334	0.336
Mn	0.005	0.005	0.004	0.005	0.005	0.005	0.005	0.005	0.005	0.004	0.005
Ca	0.024	0.024	0.025	0.024	0.048	0.032	0.031	0.031	0.044	0.031	0.094
Na	0.006	0.009	0.008	0.008	0.013	0.011	0.011	0.011	0.013	0.012	0.018
K	0.001	—	—	—	0.001	—	—	—	—	—	—
Total	4.02	4.05	4.00	4.01	4.05	4.05	4.03	4.03	4.05	4.03	4.03
Total using FeO & Fe_2O_3	4.00			4.00	4.00		4.00	4.00	4.00	4.00	4.00
Ca[e]	1.3	1.2	1.3	1.3	2.5	1.6	1.6	1.6	2.2	1.6	5.0
Mg[e]	83.2	82.7	83.3	83.1	81.7	80.5	80.6	80.6	80.0	81.2	76.9
Fe^{2+}[e]	15.5	16.1	15.4	15.6	15.8	17.9	17.8	17.8	17.8	17.2	18.1
Fe^{2+}/Mg[f]	0.186	0.194	0.196	0.187	0.194	0.222	0.220	0.221	0.222	0.212	0.235
Al_2O_3[g]	6.2			6.2	5.9			5.4	4.7	4.6	8.1
(Mg, 'Fe') SiO_3[g]	92.4			92.4	91.5			92.8	92.9	93.7	86.6
$CaSiO_3$[g]	1.4			1.4	2.6			1.8	2.4	1.7	5.3

[a] observed and bulk composition are the same.
[b] exsolved from clinopyroxene.
[c] weighted average all orthopyroxene in rock (see Table 1).
[d] observed orthopyroxene composition plus exsolved phases (see Table 1).
[e] ionic percent; total iron as Fe^{2+}.
[f] ionic ratio; total iron as Fe^{2+}.
[g] weight percent; total iron expressed as equivalent weight of Mg.
Analyst: M. H. Beeson.

O'Hara and Yoder, 1967) have tended to confirm the high pressure origin of such rocks and to set some limits on the temperature-pressure relations of garnet-pyroxene assemblages at both liquidus and subsolidus conditions.

Boyd and Nixon (1970) have recently shown that clinopyroxenes from South African garnet pyroxenites fall into calcic and subcalcic groups, and they stress the temperature, rather than pressure, dependence of these groups compared to the subsolidus relations in the system $MgSiO_3$-$CaMgSiO_3$ studied by Davis and Boyd (1966) at 30 kbar. We have plotted our bulk and reconstructed pyroxene data on Boyd and Nixon's diagram (Fig. 6). Our clino-

TABLE 5. COMPOSITIONS OF GARNETS

	68SAL-6	68SAL-24		68SAL-26		68SAL-7			68SAL-11
	Exsolved[a,b] observed	Exsolved[b,c] observed	Reacted from spinel observed	Exsolved[b,c] observed	Reacted from spinel observed	Discrete grains observed	Exsolved and reacted from spinel[d] observed	Calculated[e] Bulk	Discrete grains observed
SiO_2	41.15	41.29	40.97	41.37	41.26	41.83	40.77	41.37	40.52
Al_2O_3	23.02	23.12	23.06	23.07	23.16	22.91	22.94	22.92	22.52
'FeO'	11.20	11.85	11.97	13.17	13.29	11.09	12.95	11.90	16.33
MgO	18.06	18.32	18.25	17.99	17.89	18.49	18.00	18.28	15.78
CaO	5.44	5.12	5.07	4.84	4.87	5.27	4.69	5.02	4.93
Na_2O	0.04	n.d.	n.d.	n.d.	n.d.	n.d.	n.d.	n.d.	n.d.
K_2O	0.03	n.d.	n.d.	n.d.	n.d.	n.d.	n.d.	n.d.	n.d.
TiO_2	0.22	0.13	0.13	0.18	0.23	0.48	0.32	0.41	0.38
Cr_2O_3	n.d.	0.44	0.42	0.26	0.28	0.14	0.08	0.11	0.08
MnO	0.41	0.46	0.46	0.41	0.40	0.31	0.33	0.32	0.46
Total	99.57	100.73	100.33	101.29	101.38	100.52	100.08	100.33	101.00
Calc. FeO	9.56	9.90		10.95				10.51	13.88
Calc. Fe_2O_3	1.82	2.17		2.47				1.55	2.72
Total	99.75	100.95		101.54				100.49	101.27
Number of ions on the basis of 24 oxygens									
Si	5.955	5.925	5.908	5.929	5.913	5.983	5.907	5.951	5.917
Al^{IV}	0.045	0.075	0.092	0.071	0.087	0.017	0.093	0.049	0.084
Al^{VI}	3.881	3.834	3.827	3.826	3.824	3.845	3.825	3.836	3.792
Cr	—	0.050	0.048	0.030	0.032	0.016	0.009	0.013	0.009
Ti	0.024	0.014	0.014	0.019	0.025	0.052	0.035	0.043	0.042
Mg	3.896	3.918	3.923	3.843	3.821	3.942	3.888	3.919	3.434
Fe^{2+}	1.355	1.422	1.444	1.579	1.593	1.327	1.569	1.432	1.994
Mn	0.050	0.056	0.056	0.050	0.049	0.038	0.041	0.039	0.057
Ca	0.844	0.787	0.783	0.743	0.748	0.808	0.728	0.774	0.771
Na	0.011	—	—	—	—	—	—	—	—
K	0.006	—	—	—	—	—	—	—	—
Total	16.06	16.08	16.09	16.09	16.09	16.03	16.09	16.06	16.10
Total using FeO & Fe_2O_3	16.00	16.00		16.00				16.00	16.00
Ca[f]	13.8	12.8	12.7	12.1	12.2	13.3	11.8	12.6	12.4
Mg[f]	63.9	64.0	63.8	62.3	62.0	64.9	62.8	64.0	55.4
Fe^{2+}[f]	22.3	23.2	23.5	25.6	25.8	21.8	25.4	23.4	32.2
Fe^{2+}/Mg[g]	0.348	0.363	0.368	0.411	0.417	0.337	0.404	0.365	0.581
Al_2O_3[h]	24.2	24.1		23.9				24.0	23.7
(Mg, 'Fe') SiO_3[h]	64.0	64.9		65.7				65.2	65.6
$CaSiO_3$[h]	11.8	11.0		10.4				10.8	10.7

[a] exsolved from clinopyroxene.
[b] observed and bulk compositions are the same.
[c] exsolved from both orthopyroxene and clinopyroxene.
[d] undifferentiated.
[e] weighted average of all garnet in rock (see Table 1).
[f] ionic percent; total iron as Fe^{2+}.
[g] ionic ratio; total iron as Fe^{2+}.
[h] weight percent; total iron expressed as equivalent weight of Mg.
Analyst: M. H. Beeson.

pyroxenes also fall into two groups offset toward the iron-rich side of the quadrilateral, although the presence of a "miscibility gap" between the two sets seems less obvious from our data than theirs. Whether or not the series is continuous, all of our reconstructed pyroxenes have shifted relative to the bulk compositions in the direction of higher temperature in the synthetic system. If projected parallel to the $MgSiO_3$-$FeSiO_3$ join, our bulk clinopyroxene compositions have Ca/Ca+Mg ratios that suggest equilibration temperatures of 1050–1150°C, whereas the reconstructed compositions show that original clinopyroxene compositions would have equilibrated at temperatures

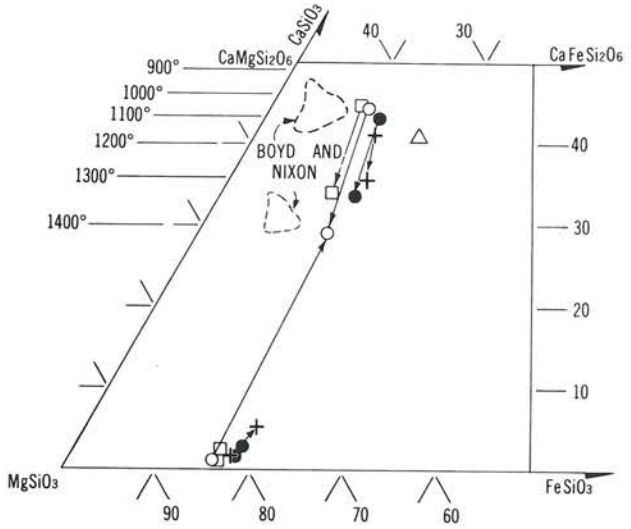

FIG. 6. Bulk and reconstructed compositions of ortho- and clinopyroxenes plotted on the pyroxene quadrilateral. Mole percent. Arrows lead from bulk to reconstructed compositions. Symbols identify sample numbers as in Fig. 4. The temperatures shown are for the diopside solvus in the system $CaMgSi_2O_6$-$MgSiO_3$ at 30 kbar (Davis and Boyd, 1966). Shaded areas show diopsidic pyroxenes from African kimberlites from Boyd and Nixon (1970).

nearer 1300–1400°C. Bulk and reconstructed compositions of orthopyroxene, plotted on the same diagram, correspond to lower and higher temperatures, respectively, in agreement with the clinopyroxenes. Actual temperatures were doubtlessly lower as a consequence of iron and Al_2O_3 in the natural system, but our texturally reconstructed phases seem to have equilibrated at higher, perhaps liquidus or solidus, temperatures, and to have been partially reequilibrated at lower, subsolidus temperatures.

Comparison of distribution coefficients of Mg and Fe^{2+} in coexisting garnet and clinopyroxene tends to show the same direction of shift. According to Banno and Matsui (1965), lower coefficients of the form

$$K' = \ln \frac{X_{Mg}^{Ga}}{X_{Fe}^{Ga}} - \ln \frac{X_{Mg}^{Cpx}}{X_{Fe}^{Cpx}}$$

correlate with higher equilibration temperatures, although Kushiro and Aoki (1969) point out that the coefficient is pressure dependent as well. Lovering and White (1969) have compiled a large number of K' values of coexisting garnet-clinopyroxene pairs to confirm this relation, and our data are plotted on their diagram in Figure 7. The bulk compositions of clinopyroxenes and garnets from our five xenoliths yield K' values that fall into the general range of Delegate and previously analyzed Salt Lakes values. The K' of the reconstructed compositions of these minerals in 68SAL-7, the one xenolith that retains both clinopyroxene and garnet in its reconstructed mode, and that also shows partial reequilibration textures, falls well toward the high-temperature (low K') side of the diagram. The position of the type 4 xenolith (68SAL-11) in this diagram suggests that it too may have reequilibrated slightly, although it shows no textural evidence of having done so. On the other hand, it is the only one of our xenoliths without orthopyroxene, which may affect its distribution coefficient.

Irving and Green (1969) suggest that unmixing textures occur in garnet pyroxenites with 100 $Mg/Mg+Fe^{2+}$ ratios greater than 85; presumably, more iron-rich compositions have different subsolidus behavior. Our xenoliths show unmixing at 100 $Mg/Mg+Fe^{2+}$ ratios as low as 81 (Table 2). We cannot say whether the absence of exsolution textures in 68SAL-11 is due to high iron content, lack of reequilibration, or both.

Applications from experimental studies. Green (1966) has proposed that the Honolulu garnet pyroxenites are cumulates produced by fractional crystallization of an alkali olivine basalt magma at about 18 kbar pressure. Green's diagram illustrating the process is reproduced here as Figure 8. At about 18 kbar, Al-rich clinopyroxene on the liquidus, if accumulated and cooled to about 1000°C, would yield a subsolidus assemblage of pyroxene and garnet, which would then be carried upward by ascending basalt. Alternatively, it seems to us that a high temperature monomineralic Al-rich clinopyroxenite could be generated by fractional fusion as well as by fractional crystallization. Also, we question the restricted temperature and pressure range permitted by Green for both liquidus and subsolidus assemblages. The bulk chemistry of our type 4 xenolith is much more similar to Bultitude and Green's (1967) olivine

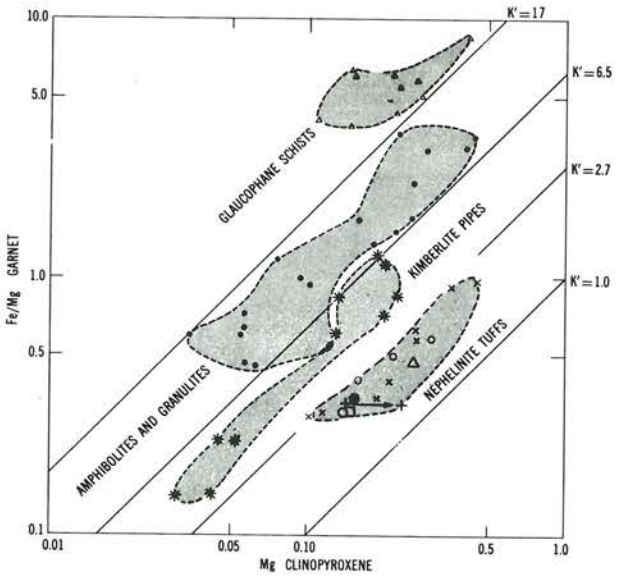

FIG. 7. Log-log distributions of Fe/Mg between coexisting garnet and clinopyroxene from various environments (modified from Lovering and White, 1969). Large symbols (circles, squares, pluses, etc.) identify sample numbers and are the same as in Fig. 4. Arrow leads from bulk to reconstructed compositions (only one of our samples contained both garnet and clinopyroxene in the reconstructed mode).

nephelinite, than to Green and Ringwood's (1967a) alkali olivine basalt. In the high pressure liquidus and solidus relations (dry) of Bultitude and Green's olivine nephelinite, clinopyroxene does not appear on the liquidus until 22.5 kbar, and a similar accumulation theory with clinopyroxene on the liquidus and garnet near the solidus would require pressures of about 27 kbar. Similarly, small changes in bulk chemistry between three Delegate xenoliths investigated at high temperature and pressure by Irving and Green (1969) seem to result in very large differences in assemblages at any given set of T-P conditions. We argue with O'Hara (1969), that Green's (1966) conditions of temperature and pressure are too restrictive.

To follow another approach, we plotted our bulk mineral compositions on Boyd's (1970) experimentally determined subsolidus system $CaSiO_3$-$MgSiO_3$-Al_2O_3 at 1200°C, a portion of which is shown in Figure 9. The three-phase field defined by the observed mineral assemblages of four of our xenoliths corresponds remarkably well with the three-phase field of the experimental system, considering that all our minerals contain iron. The two-phase tie line of our type 4 xenolith lies slightly to the right of its expected position, perhaps a result of different conditions of partial reequilibration, or a lack of them. The presence of iron in the natural system would suggest an actual subsolidus temperature less than 1200°C; on the other hand, the Al_2O_3 content of the natural clinopyroxenes is greater than those of the pure Mg system, which would indicate a somewhat higher equilibration temperature. For the present, we can only conclude that the garnet pyroxenite xenoliths reequilibrated at temperatures and pressures somewhere near those of the experimental system.

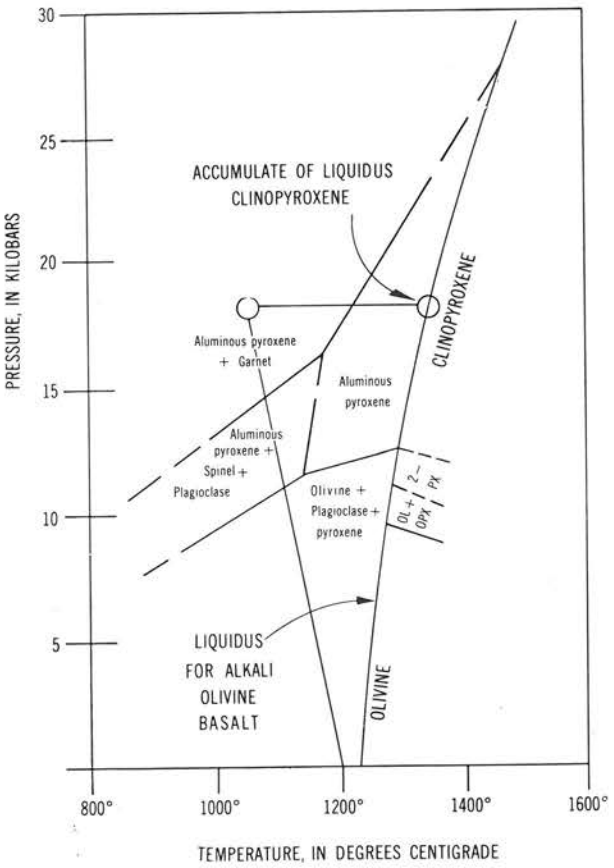

FIG. 8. Diagram showing the estimated P-T fields for different mineral assemblages in rocks with the chemical composition of the Salt Lake Crater garnet pyroxenites. After Green (1966).

Inasmuch as our bulk mineral assemblages and compositions, which we regard as having been formed during subsolidus reequilibration, fit the experimentally determined subsolidus relations fairly well, we attempted to test our reconstructed assemblages and compositions against the liquidus relations in this system. The liquidus and solidus relations in the system $CaSiO_3$-$MgSiO_3$-Al_2O_3 have not been determined directly at 30 kbar, but the part of major interest to us can be pieced together from the $CaMgSiO_3$-$Mg_3Al_2Si_3O_{12}$ join (O'Hara, 1963; O'Hara and Yoder, 1967), the $MgSiO_3$-$Mg_3Al_2Si_3O_{12}$ join (Boyd and England, 1964), and the $CaMgSiO_2$-$MgSiO_3$ join (Davis and Boyd, 1966), all investigated at 30 kbar. We have combined the available data in Figures 10 and 11. It is apparent that with increasing temperature, the three phase region of the diagram is much diminished and the fields of diopside and enstatite solid solution are much expanded. It would not appear, from existing data, that pigeonite occurs as a complicating phase, although Kushiro (1969) found that mineral at the solidus on the join $CaMgSiO_3$-$MgSiO_3$ at 20 kbar. Davis and Boyd did not identify pigeonite in the system at 30 kbar, and, even if missed, there is no evidence that it extends out into the three phase area.[1]

Presnall (1969) has recently pointed out that fractional crystallization and fractional fusion are not reversible processes in complex systems, but may lead to different solid products and derived liquids. We therefore calculated fractional crystallization paths (Bowen, 1941) on Figure 10 and fractional fusion paths (Presnall, 1969) on Figure 11. It is apparent from Figure 10 that a liquid capable of fractionally crystallizing aluminous clinopyroxene like that of our type 1 xenolith, will, with perfect fractionation, later yield orthopyroxene-rich websterites, and finally, garnet clinopyroxenites. If intercumulus liquids were trapped among the cumulates, the bulk compositions of the pyroxene cumulates would shift slightly toward the Al_2O_3 corner, but would not change greatly. During this process, mineral compositions would be expected to change in the direction shown by the arrows. It is an interesting point that, in the ternary system, almost no volume of three-phase rock would be expected on perfect fractional crystallization; the liquid composition should pass the ternary reaction point without pause. This effect would, of

[1] Nor is there any evidence that pigeonite is, or was, a constituent of our xenoliths. It has been diligently looked for, but not found (Malcolm Ross, pers. commun., 20 Dec. 1969).

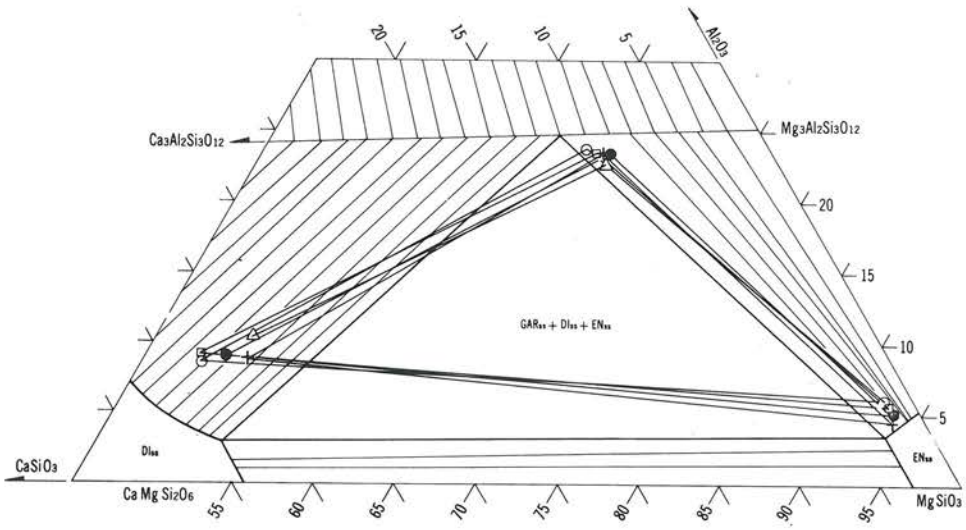

FIG. 9. Synthesis diagram for phase relations in a portion of the system $CaSiO_3$-$MgSiO_3$-Al_2O_3 at 30 kbar and 1200°C. After Boyd (1970). Weight percent. DI, diopside; GAR, garnet; EN, enstatite; subscript ss indicates solid solution. Large symbols connected by tie lines show bulk mineral compositions of our xenoliths. Symbols identify sample numbers as in Fig. 4.

course, be reduced to an unknown extent by the addition of more components in the natural system.

This portion of the $CaSiO_3$-$MgSiO_3$-Al_2O_3 system behaves differently if it is fractionally fused (Fig. 11). Parental material lying near the pyroxene-rich side of the liquidus in the garnet-clinopyroxene field (like our type 4 xenoliths), will, with perfect fractional fusion, yield residua of garnet clinopyroxenite, garnet websterite, clinopyroxene-rich websterite, and, finally clinopyroxenite. In this particular system, the liquid path will change smoothly, but will pause at the ternary reaction point and should yield a relatively large supply of liquid of that composition. Mineral compositions during fractional fusion will change along the same trends, but in the opposite directions from those in the fractionally crystallizing system.

The system nicely illustrates Presnall's (1969) point that fractional crystallization, in general, leads to continuously changing liquids and to chemically disconnected cumulates, whereas fractional fusion, in general, leads to chemically discontinuous liquids and to residua continuous

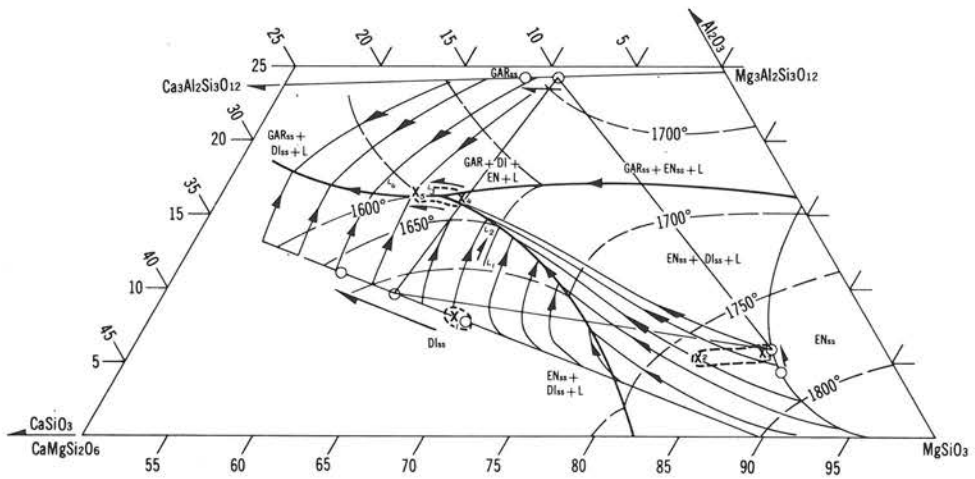

FIG. 10. Fractional crystallization paths in a portion of the system $CaSiO_3$-$MgSiO_3$-Al_2O_3 at 30 kbar. Weight percent. Data sources: the join $CaMgSi_2O_6$-$MgSiO_3$, Davis and Boyd (1966); the join $MgSiO_3$-$Mg_3Al_2Si_3O_{12}$, Boyd and England (1964); the join $CaMgSi_2O_6$-$Mg_3Al_2Si_3O_{12}$, O'Hara (1963) and O'Hara and Yoder (1967). Heavy lines are liquidus paths, dashed lighter lines are isotherms; solid light curved lines are liquidus fractionation lines (Bowen, 1941). *L*, liquid; other abbreviations as in Fig. 9. Liquids fractionating along the paths L_1-L_2 produce cumulates of bulk composition X_1; liquids along the path L_2-L_3, cumulates of composition X_2-X_3; liquids along the path L_3-L_4, cumulates of X_4-X_5. Liquid compositions change continuously; cumulate compositions discontinuously. Mineral compositions change in the direction indicated by arrows during fractional crystallization.

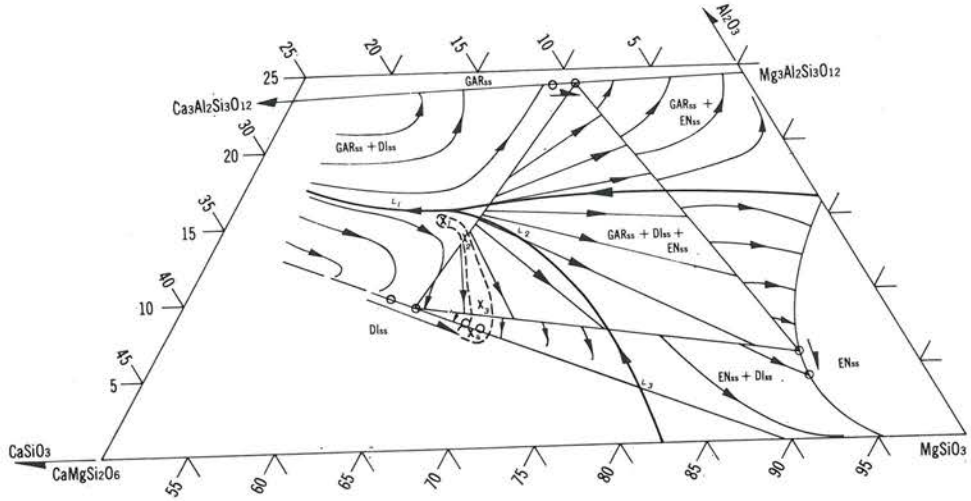

FIG. 11. Fractional fusion paths in a portion of the system $CaSiO_3$-$MgSiO_3$-Al_2O_3 at 30 kbar. Weight percent. Sources and abbreviations same as in Fig. 9. Solid light curved lines are solidus fractionation lines (Presnall, 1969). Solids fusing along the path X_1-X_2-X_3-X_4 produce liquids of compositions L_1-L_2. Solid residua change composition continuously; liquid compositions are continuous in this portion of the system as well. Mineral compositions change in the direction indicated by the arrows during fractional fusion.

in bulk chemistry. In the $CaSiO_3$-$MgSiO_3$-Al_2O_3 system, the dominant process would most likely be identified by bulk chemistry of liquids and solid products; the mineral chemistry shows the same trends for either process.

The natural system. To test these models against the natural system of Honolulu liquids and xenoliths, we recalculated the compositions of 37 analyzed Honolulu basalts (sources from Jackson and Wright, in press) and plotted them on an iron-bearing variant of the experimentally determined system (Fig. 12). The natural data seem to show a shifting set of liquidus paths defined by the SiO_2 content of the basalts. The good definition of liquidus paths by basalt type was as surprising as the apparent shift, but whether the latter is caused by pressure or source chemistry is unknown. It is also difficult to evaluate whether the compositional plots bunch in such a way as to suggest a reaction point—the silica-poor melilite-nepheline basalts show little evidence of this, for example, but those of basanitic composition may. Since our analyzed type 4 xenolith (whose bulk chemistry is closest to Honolulu liquid compositions) has basanitic affinities, we selected the liquidus path defined by basalts with 42–44 percent SiO_2 as the one with which to compare our xenolith compositions.

Figure 13 shows the natural system as well as we can construct it from our compositional data. The three-phase

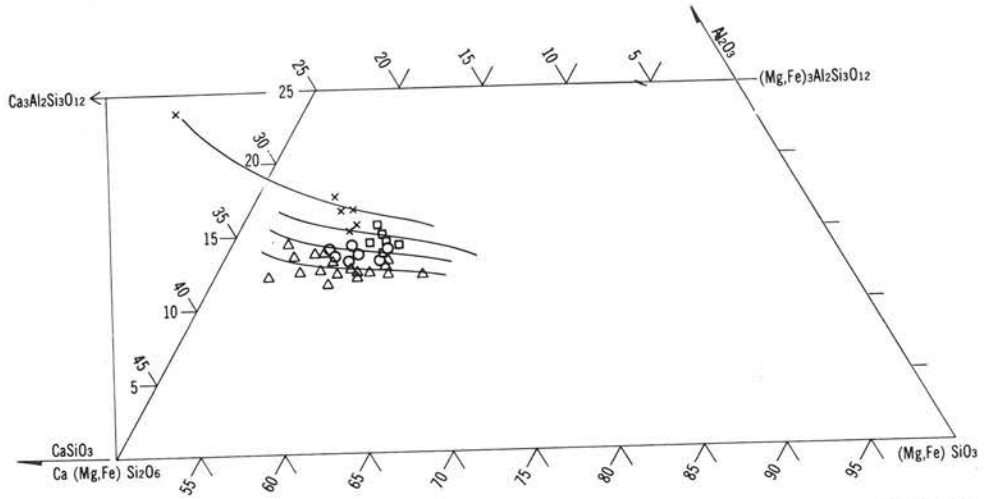

FIG. 12. Liquidus paths for basalts of the Honolulu Volcanic Series plotted in a portion of the system $CaSiO_3$-$(Mg,Fe)SiO_3$-Al_2O_3. Weight percent; total iron expressed as equivalent weight of Mg. Sources of data same as Jackson and Wright (1970). *X*'s are alkali olivine basalts (>44% SiO_2); squares are basanites (42–44 percent SiO_2); circles, nepheline basalts (40–42 percent SiO_2); triangles, melilite-nepheline basalts (<40 percent SiO_2). Light solid lines are presumed natural liquidus paths.

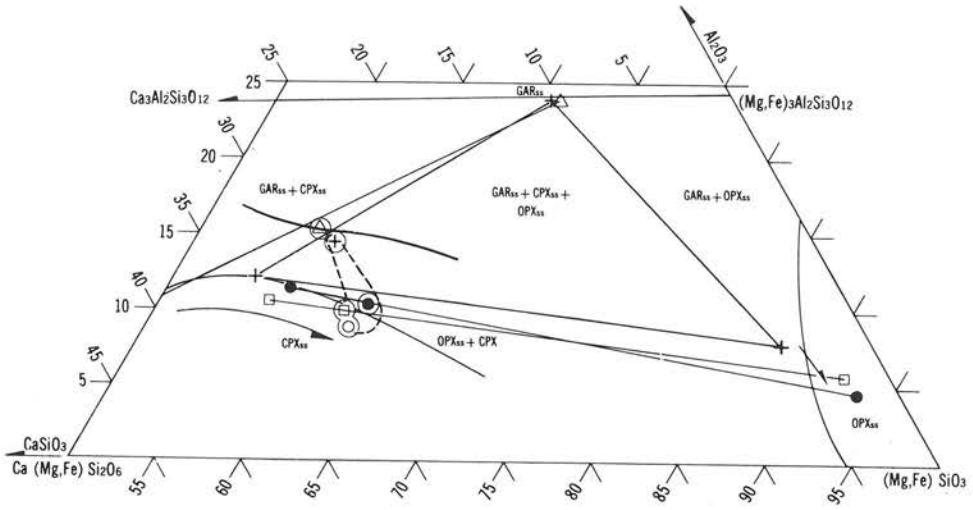

FIG. 13. Reconstructed fractional fusion paths in a portion of the system $CaSiO_3$-$(Mg,Fe)SiO_3$-Al_2O_3. Weight percent; total iron expressed as equivalent weight of Mg. Heavy line indicates basanite liquidus from Fig. 12. CPX, clinopyroxene; OPX, orthopyroxene; other abbreviations as in Fig. 10. Symbols for whole rock xenolith compositions and reconstructed mineral analyses are the same as those of Fig. 4. The reconstructed mineral compositions of 68SAL-7 define the three phase field. The whole rock compositions define a path of continuous bulk chemical change similar to that of Fig. 11. Changes in reconstructed mineral chemistry are shown by arrows.

field, defined by the reconstructed mineral compositions of the type 3 xenolith, is remarkably like that of the experimental system. The reconstructed mineral compositions of the type 1, 2, and 4 xenoliths define the pyroxene solid solution fields.[1] Clinopyroxene solid solutions trend between $MgSiO_3$ and Ca-Tschermak's molecule, and the orthopyroxene solid solutions show considerable spread in Al_2O_3 content; both minerals behave as predicted in the fractional crystallization or fractional fusion models of the experimental system. Garnet solid solutions, however, show little change. The basanitic garnet clinopyroxene (type 4) xenolith plots on the liquidus and tends to confirm our suspicion that this xenolith was a liquid equilibrated at high T–P conditions. The continuous changes in whole-rock chemistry of the xenoliths and the absence of orthopyroxene-rich xenoliths predicted by the fractional crystallization model strongly suggest an origin by fractional fusion for the type 1, 2, and 3 rocks.

The Honolulu liquid compositions, the reconstructed mineral compositions, and the whole-rock xenolith compositions all fit the $CaSiO_3$-$MgSiO_3$-Al_2O_3 system at 30 kbar fairly well, as do the subsolidus assemblages. Due to the presence of iron in the system, and a lack of knowledge as to how fast the system changes with pressure, we cannot, to be sure, put firm numbers on the pressures at which these liquids and xenoliths originated, but a range around 30 kbar is suggested as a first estimate.

[1] It is encouraging to note that our type 1 and 2 xenoliths, which contain only unmixed garnet, when plotted on O'Hara (1968; 1969) type CS-MS-A diagrams, fall on the undersaturated side of his limit of garnet solubility in clinopyroxene curve determined by O'Hara and Yoder (1967) at 30 kbar; whereas our type 3 and 4 xenoliths, which contain original garnet, fall on the Al_2O_3-rich side as predicted.

CONCLUSIONS

The garnet pyroxenite xenoliths in the Honolulu Volcanic Series are clearly related chemically to the undersaturated basalts that contain them, and not to the copious tholeiites that build the major parts of the Hawaiian shields. They appear to represent liquids, parents, and residua related to the partial melting that produced the Honolulu magmas at considerable depth (perhaps around 100 km) in the mantle beneath Oahu. After forming at liquidus to solidus temperatures, the xenoliths were held at lower temperatures, but not necessarily lower pressures, for some time before being broken loose and incorporated as xenoliths in the Honolulu basalts. During this period, they partially reequilibrated, which resulted in considerable unmixing and reaction of phases. Fractional crystallization does not seem to have been an important process in their origin; cumulus textures are lacking, and the proportions of phases present in the xenoliths are different from those expected for mantle cumulates of their composition.

The garnet pyroxenites are interbanded with lherzolites at depth. Whether those garnet pyroxenites near liquidus compositions ultimately originated by partial fusion of pyroxene-rich lherzolites, or whether they represent preexisting mantle rocks, they appear to have been themselves partially fused before and during Honolulu magma production. The volume of the rocks represented by these xenoliths at depth is unknown. The volume of undersaturated basalt in Hawaii is relatively small; even if a large amount of garnet-rich material were available at depth that was potentially parental to such basalts, the volume of clinopyroxene-rich residua would not be greater than one to four times the volume of basalt produced.

Finally, we would like to stress that we are reporting

here on only one set of the great variety of xenoliths contained in Hawaiian basalts. In addition to a large suite of plagioclase-bearing crustal cumulates, there are several other suites of rocks believed to be mantle residents—a large group of dunite-wehrlites, abundant olivine-rich lherzolites, and a suite of garnet lherzolites to name but three. As work continues on the compositions and processes involved in the mantle samples, compositions seem to be increasingly heterogeneous, and processes seem increasingly diverse. We see no reason to suppose that the rocks of the mantle beneath the Hawaiian chain are any less heterogeneous than the rocks of the crust.

ACKNOWLEDGEMENTS

We are very grateful to our colleagues E. H. Roseboom and H. G. Wilshire for critically reviewing the manuscript. We are especially indebted to D. C. Presnall for his help and comments in evaluating fractional crystallization and fusion paths in a portion of the system $CaSiO_3$-$MgSiO_3$-Al_2O_3.

REFERENCES

BANNO, SHOHEI, AND YOSHITO MATSUI (1965) Eclogite types and partition of Mg, Fe, and Mn between clinopyroxene and garnet. *Proc. Jap. Acad.* **41,** 716–721.

BEAMAN, D. R., AND J. A. ISASI (1970) A critical examination of computer programs used in quantitative electron microprobe analysis. *Anal. Chem.* in press.

BEESON, M. H. (1967) A computer program for processing electron microprobe data. *U.S. Geol. Surv. Open-File Rep.*

BOWEN, N. L. (1941) Certain singular points on crystallization curves of solid solutions. *Proc. Nat. Acad. Sci.* **27,** 301–309.

BOYD, F. R. (1969) Electron-probe study of diopside inclusions from kimberlite. *Amer. J. Sci.* **267A,** 50–69.

———, (1970) The system $CaSiO_3$-$MgSiO_3$-Al_2O_3. *Carnegie Inst. Wash. Year Book* **68,** 214–221.

———, AND J. L. ENGLAND (1964) The system enstatite-pyrope. *Carnegie Inst. Wash. Year Book* **63,** 157–161.

———, AND P. H. NIXON (1970) Kimberlite diopsides. *Carnegie Inst. Wash. Year Book* **68,** 324–329.

BULTITUDE, R. J., AND D. H. GREEN (1967) Experimental study at high pressures on the origin of olivine nephelinite and olivine melilite nephelinite magmas. *Earth Planet. Sci. Lett.* **3,** 325–337.

DAVIS, B. T. C. (1963) The system enstatite-diopside at 30 kilobars pressure. *Carnegie Inst. Wash. Year Book* **62,** 103–107.

———, AND F. R. BOYD (1966) The join $Mg_2Si_2O_6$–$CaMgSi_2O_6$ at 30 kilobars pressure and its application to pyroxenes from kimberlites. *J. Geophys. Res.* **71,** 3567–3576.

DICKEY, J. S., JR. (1968) Eclogitic and other inclusions in the Mineral Breccia member of the Deborah Volcanic Formation at Kakanui, New Zealand. *Amer. Mineral.* **53,** 1304–1319.

——— (1970) Partial fusion products in alpine-type peridotites: Serrania de la Ronda and other examples. *Mineral Soc. Amer. Spec. Pap.* **3,** 33–49.

GIROD, M. (1967) Données pétrographiques sur des pyroxenolites á grenat en enclaves dans des basaltes du Haggar (Sahara Central). *Bull. Soc. Franc. Mineral. Cristallogr.* **90,** 202–213.

GOODRICH, JOSEPH (1826) Notice of the volcanic character of the Island of Hawaii. *Amer. J. Sci.* **11,** 1–36.

GREEN, D. H. (1966) The origin of the "eclogites" from Salt Lake Crater, Hawaii. *Earth Planet. Sci. Lett.* **1,** 414–420.

———, AND A. E. RINGWOOD (1967a) An experimental investigation of the gabbro to eclogite transformation and its petrological applications. *Geochim. Cosmochim. Acta* **31,** 767–833.

———, AND ——— (1967b) The genesis of basaltic magmas. *Contrib. Mineral. Petrology* **15,** 103–190.

HITCHCOCK, C. H. (1900) Geology of Oahu. *Geol. Soc. Amer. Bull.* **11,** 15–60.

IRVING, A. J., AND D. H. GREEN (1969), Experimental duplication of mineral assemblages in basic inclusions of the Delegate Breccia Pipes. *Phys. Earth Planet. Inter.* **3,** 385–389.

JACKSON, E. D. (1966) "Eclogite" in Hawaiian basalts. *U.S. Geol. Surv. Prof. Pap.* **550-D,** D151–D157.

———, (1968) The character of the lower crust and upper mantle beneath the Hawaiian Islands. *Int. Geol. Congr. 23rd, Prague, Proc.* **1,** 135–150.

JACKSON, E. D., AND T. L. WRIGHT (1970) Xenoliths in the Honolulu Volcanic Series, Hawaii. *J. Petrology.* **11,** 405–430.

KORNPROBST, J. (1969) Le massif ultrabasique des Beni Bouchera (Rif Interne, Maroc): Etude des péridotites de haute température et de haute pression, et des pyroxénolites, à grenat ou sans grenat, qui leur sont associées. *Contrib. Mineral. Petrology* **23,** 283–322.

KUNO, HISASHI (1964) Aluminian augite and bronzite in alkali olivine basalt from Taka-Sima, North Kyusyu, Japan. *In Advancing Frontiers in Geology and Geophysics,* Osmania Univ. Press (India), 205–220.

———, (1969) Mafic and ultramafic nodules in basaltic rocks of Hawaii. *Geol. Soc. Amer. Mem.* **115,** 189–233.

KUSHIRO, IKUO (1969) Synthesis and stability of iron-free pigeonite in the system $MgSiO_3$-$CaMgSi_2O_6$ at high pressures. *Carnegie Inst. Wash. Year Book* **67,** 80–83.

———, AND KEN-ICHIRO AOKI (1968) Origin of some eclogite xenoliths in kimberlite. *Amer. Mineral.* **53,** 1347–1367.

———, AND H. S. YODER, JR. (1966) Anorthite-forsterite and anorthite-enstatite reactions and their bearing on the basalt-eclogite transformation. *J. Petrology* **7,** 337–362.

LOVERING, J. F., AND A. J. R. WHITE (1969) Granulitic and eclogitic inclusions from basic pipes at Delegate, Australia. *Contrib. Mineral. Petrology* **21,** 9–52.

MACDONALD, G. A., AND T. KATSURA (1964) Chemical composition of Hawaiian lavas. *J. Petrology* **5,** 82–133.

MACGREGOR, I. D. (1969) The genesis of eclogite xenoliths from the Roberts Victor Kimberlite pipe, South Africa [abstr.]. *EOS, Trans. Amer. Geophys. Union* **50,** 342.

MCDOUGALL, IAN (1964) Potassium-argon ages from lavas of the Hawaiian Islands. *Geol. Soc. Amer. Bull.* **75,** 107–128.

MASON, BRIAN (1966) Pyrope, augite, and hornblende from Kakanui, New Zealand, *N. Z. J. Geol. Geophys.* **9,** 474–480.

O'HARA, M. J. (1963) The join diopside-pyrope at 30 kilobars. *Carnegie Inst. Wash. Year Book* **62,** 116–119.

———, (1968) The bearing of phase equilibria studies in synthetic and natural systems on the origin and evolution of basic and ultrabasic rocks. *Earth Sci. Rev.* **4,** 69–133.

———, (1969) The origin of eclogite and ariegite nodules in basalt. *Geol. Mag.* **106,** 322–330.

———, AND H. S. YODER, JR. (1967) Formation and fractionation of basic magmas at high pressures. *Scott. J. Geol.* **3,** 67–117.

PECK, L. C. (1964) Systematic analysis of silicates. *U.S. Geol. Surv. Bull.* **1170,** 89 p.

PRESNALL, D. C. (1969) The geometrical analysis of partial fusion. *Amer. J. Sci.* **217,** 1178–1194.

RICKWOOD, P. C., M. MATHIAS, AND J. C. SIEBERT (1968) A study of garnets from eclogite and peridotite xenoliths found in Kimberlite. *Contrib. Mineral. Petrology* **19,** 271–301.

SAGGERSON, E. P. (1968) Eclogite nodules associated with alkaline olivine basalts, Kenya. *Geol. Rundsch.* **57,** 890–903.

STEARNS, H. T., AND K. N. VAKSVIK (1935) Geology and ground water resources of the Island of Oahu, Hawaii. *Hawaii Div. Hydrogr. Bull.* **1,** 479 p.

TILLEY, C. E., AND H. S. YODER, JR. (1964) Pyroxene fractionation in mafic magma at high pressures and its bearing on basalt genesis. *Carnegie Inst. Wash. Year Book* **63,** 114–121.

WHITE, R. W. (1966) Ultramafic inclusions in basaltic rocks from Hawaii. *Contrib. Mineral. Petrology* **12,** 245–314.

WRIGHT, T. L., AND P. DOHERTY (1970) A linear programming and least squares computer method for solving petrologic mixing problems. *Geol. Soc. Amer. Bull.* (in press.)

YODER, H. S., JR. AND C. E. TILLEY (1962) Origin of basaltic magmas: an experimental study of natural and synthetic rock systems. *J. Petrology* **3,** 342–532.